

Communication

A Pragmatic and High-Performance Radiative Cooling Coating with Near-Ideal Selective Emissive Spectrum for Passive Cooling

Mingxue Chen ^{1,2}, Wenqing Li ^{1,2}, Shuang Tao ^{1,2}, Zhenggang Fang ^{1,2,*}, Chunhua Lu ^{1,2,3,*} and Zhongzi Xu ^{1,2,3}

¹ State Key Laboratory of Materials-Oriented Chemical Engineering, College of Materials Science and Engineering, Nanjing Tech University, Nanjing 210009, China; cmx2017@njtech.edu.cn (M.C.); wengqingli@njtech.edu.cn (W.L.); 201861103165@njtech.edu.cn (S.T.); zzzxu@njtech.edu.cn (Z.X.)

² Jiangsu Collaborative Innovation Center for Advanced Inorganic Function Composites, Nanjing Tech University, Nanjing 210009, China

³ Jiangsu National Synergetic Innovation Center for Advanced Materials (SICAM), Nanjing Tech University, Nanjing 210009, China

* Correspondence: zgfang@njtech.edu.cn (Z.F.); chhlu@njtech.edu.cn (C.L.)

Received: 16 December 2019; Accepted: 24 January 2020; Published: 5 February 2020



Abstract: Radiative cooling is a passive cooling technology that can cool a space without any external energy by reflecting sunlight and radiating heat to the universe. Current reported radiative cooling techniques can present good outside test results, however, manufacturing an efficient radiative material which can be applied to the market for large-scale application is still a huge challenge. Here, an effective radiative cooling coating with a near-ideal selective emissive spectrum is prepared based on the molecular vibrations of SiO_x, mica, rare earth silicate, and molybdate functional nanoparticles. The radiative cooling coating can theoretically cool 45 °C below the ambient temperature in the nighttime. Polyethylene terephthalate (PET) aluminized film was selected as the coating substrate for its flexibility, low cost, and extensive production. As opposed to the usual investigations that measure the substrate temperature, the radiative cooling coating was made into a cubic box to test its space cooling performance on a rooftop. Results showed that a temperature reduction of 4 ± 0.5 °C was obtained in the nighttime and 1 ± 0.2 °C was achieved in the daytime. Furthermore, the radiative cooling coating is resistant to weathering, fouling, and ultraviolet radiation, and is capable of self-cleaning due to its hydrophobicity. This practical coating may have a significant impact on global energy consumption.

Keywords: radiative cooling coating; selective emissive spectrum; flexibility; low-cost; extensive production; hydrophobicity

1. Introduction

Cooling, as one of the major end-uses of energy globally and a major driver of peak electricity demand, has attracted considerable attention in recent years. For example, air conditioning consumes about 15% of the total primary energy used by American commercial buildings and 70% of total electricity consumption in Saudi Arabia [1,2]. In India, residential buildings consume 45% of the energy to maintain the conditions of thermal comfort [3]. Therefore, passive cooling could have a significant impact on global energy consumption for its ability to cool without external energy. Efficient radiative cooling devices are expected to exhibit a thermal radiative peak within 8 to 13 μm, which is known as the atmospheric window, in order to transfer the heat directly to outer space [4–6]. Radiative cooling technologies have been extensively investigated in the last decades [7–9]. However, although most

technologies present outside test results, manufacturing a radiative cooling material which can be implemented into the complex urban environment of crowded buildings is still a challenge.

If an efficient radiative material can be applied to the market for large-scale application (for example, buildings, curtains, and tents), the following characteristics should be exhibited [10,11]: (1) it has a near-ideal emittance profile, (2) it has a good cooling effect, (3) the substrate should be rigid or flexible, (4) it can be put into extensive production, and (5) the price is affordable.

In this work, an efficient radiative cooling coating with a near-ideal selective emissive spectrum is reported, which can meet the five characteristics above for market application. Due to the Si–O–Si asymmetric vibrations of SiO_x (8–10 μm) [12], the B–O stretching vibration of mica (10–11 μm) [13], the Si–O stretching vibration modulated by rare earth ions (10–12 μm) [14], and the Mo–O stretching mode of molybdate (12–13 μm) [15], the four functional nanoparticles were embedded in the poly(vinylidene fluoride-co-hexafluoropropene) (P(VDF-HFP)) coating to match well with the entire atmosphere window (8–13 μm). The P(VDF-HFP) composite coating exhibits excellent optical properties to meet the characteristics (1,2). To satisfy the characteristics (3–5), PET aluminized film is selected as the coating substrate due to being flexible, cheap, and mass-manufactured, and its ability to be applied to various fields. The composite coating was made into a cubic box to test its space cooling performance on a rooftop. It is worth noting that the radiative cooling coating showed a temperature reduction of 4 ± 0.5 °C in the nighttime. Compared with the recently published radiative cooling material based on PET substrates [10], the radiative cooling coating proposed in this work shows a better cooling performance, and is easier to fabricate at a much lower price for commercial availability.

2. Materials and Methods

2.1. PET Aluminized Film Substrate

PET aluminized film was purchased from Guangdong Yongsheng Packaging Materials Co. Ltd. (Guangzhou, China). To ensure sufficient tensile strength, PET aluminized film with a thickness of 50 μm was selected. The surface features of the PET aluminized film are shown in Figure S1a,b.

2.2. Preparation of the Radiative Cooling Coating

The preparation of the radiative cooling coating is illustrated in Figure 1. Firstly, 2 g of P(VDF-HFP) raw material (Sigma-Aldrich, Shanghai, China) was dissolved in 35 g acetone to form the P(VDF-HFP) solution. Then, 2 g deionized water was added into the solution to make a P(VDF-HFP)-acetone-water precursor solution. Next, 0.2 g SiO_x (Aladdin Chemicals, Shanghai, China), 0.6 g mica (Mineral Products, Shijiazhuang, China), 0.8 g rare earth silicate, and 0.2 g molybdate nanoparticles were added to the precursor solution. After ball-milling for 24 h, the nanoparticles were randomly dispersed into the precursor solution. Finally, the disperse system was used to produce the radiative cooling coating on a PET aluminized film by blade coating. The obtained coating was coated evenly onto the PET aluminized film and was white in color.

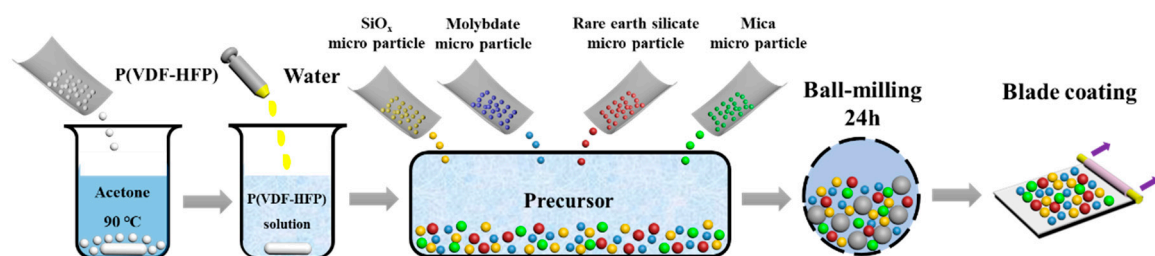


Figure 1. Schematic of the preparation process of the radiative cooling coating.

2.3. Characterization

A scanning electron microscope (SEM, Hitachi SU8010, Tokyo, Japan) and an energy dispersive spectrometer (EDS, Hitachi SU8010) were used to study the surface features of the PET aluminized film. The UV-VIS-NIR spectrometer (SHIMADZU, Kyoto, Japan) was used to measure the reflectance spectrum in the 0.3–2.5 μm wavelength range. The infrared transmission spectra, and the reflectance spectra in the wavelength range of 2.5–20 μm , were acquired by a Fourier transform infrared spectrometer (FT-IR, Frontier, PerkinElmer LLC, Waltham, MA, USA).

Rooftop measurements were carried out on 23 and 29 July 2019 in Nanjing, China (with a clear sky and relative air humidity of 84% and 65%, respectively). The prepared radiative cooling surface was placed on a polystyrene foam cubic frame ($40 \times 40 \times 40 \text{ cm}^3$ in size). The polystyrene foam was put between the cubic frame and the ground of the roof, in order to suppress the conductive heat from the ground. For comparison, two more test samples were prepared in which the PET aluminized film was coated with commercial cooling coating (Reference Sample 1, broadband radiator) and PET aluminized film (Reference Sample 2). All the sensors were calibrated previously, and the measuring errors were less than 0.2 $^{\circ}\text{C}$. Furthermore, the sensors were placed in the center of the polystyrene foam square frame and outside of that, to measure the internal temperature and ambient temperature, respectively. The solar irradiance was measured using the optical power density meter (Newport Power Meter). This test device maximally simulated the actual application environment.

3. Results and Discussion

3.1. Theoretical Cooling Performance

When the radiative cooling coating is exposed to the outside environment, it is subject to both solar irradiance and atmospheric thermal radiation. To numerically evaluate the theoretical cooling performance of samples, the net cooling power of a radiative cooler (P_{net}) could be calculated as follows [16]:

$$P_{\text{net}} = P_{\text{r}} - P_{\text{a}} - P_{\text{nonrad}} - P_{\text{sun}} \quad (1)$$

where

$$P_{\text{r}} = 2\pi \int_0^{\pi/2} \sin \theta \cos \theta d\theta \int_0^{\infty} B(T_{\text{r}}, \lambda) e_{\text{r}}(\lambda, \theta) d\lambda \quad (2)$$

is the radiative output power of the coating.

$$P_{\text{a}} = 2\pi \int_0^{\pi/2} \sin \theta \cos \theta d\theta \int_0^{\infty} B(T_{\text{a}}, \lambda) e_{\text{a}}(\lambda, \theta) e_{\text{r}}(\lambda, \theta) d\lambda \quad (3)$$

can be used to find the amount of the incident radiation power absorbed by the coating.

In the above formula, $B(T, \lambda) = \frac{2hc^2}{\lambda^5 (e^{\frac{hc}{\lambda kT}} - 1)}$ is the spectral radiance of a blackbody at temperature T , where C represents the speed of light, h represents the Planck constant, K represents the Boltzmann constant, and λ represents the wavelength. According to Kirchhoff's law, the emissivity of the cooling coating is equal to its absorptivity $e_{\text{r}}(\lambda, \theta)$. The angle-dependent emissivity of the atmosphere is $e_{\text{a}}(\lambda, \theta)$, which was defined by $e_{\text{a}}(\lambda, \theta) = 1 - t(\lambda)^{1/\cos \theta}$ [17].

In Equation (1), P_{nonrad} is nonradiative heating power which comes from the coating from the surrounding media, which can be defined as:

$$P_{\text{nonrad}} = q (T_{\text{a}} - T_{\text{r}}) \quad (4)$$

Here, $q = q_{\text{conduct}} + q_{\text{convection}}$ is the combined nonradiative heat coefficient taking root in the conductive and convective heat exchange of the coating with the surrounding air. From previous

studies, we can see that q varies from 0 to $6.9 \text{ W m}^{-2} \text{ K}^{-1}$ with the change of environment and testing equipment [6,18].

The last one on the right side of Equation (1) is the solar power absorbed by the coating, which can be defined as

$$P_{\text{sun}} = \int_0^{\infty} e_r(\lambda, \theta_{\text{sun}}) I_{\text{AM} 1.5}(\lambda) d\lambda \quad (5)$$

$e_r(\lambda, \theta_{\text{sun}})$ is the absorptivity of the coating, which has a bearing on the solar incident angle θ_{sun} .

The daytime cooling power of a cooling coating is illustrated in Equation (1). If a positive value of P_{net} is achieved in the initial state ($T_a = T_r$), the coating can be defined by a daytime cooling film. Moreover, the temperature difference $T_a - T_r$ is expected to reach a steady state when the outgoing power keeps balance with the absorbed incoming power ($P_{\text{net}} = 0$), which means there is no extra power for the coating to further cool down. Consequently, the value of $T_a - T_r$ in a steady state can be used to carry out the quantitative study on the cooling performance of the coating.

The performance of the radiative cooling coating is closely related to the spectral emissivity. Broadband and selective radiators are the two main radiators in the study of existing radiators, and their infrared emission spectra are shown in Figure 2a. While the broadband radiator has emissivity like a blackbody within the entire middle-infrared band, the selective radiator comprises unity emission only within the wavelengths of 8–13 μm which selectively spans over the atmospheric window. Figure 2b shows that the theoretical cooling performance of the selective radiator is vastly superior to that of a broadband radiator. The ambient temperature was set to 300.15 K and both the conductive and convective heat transfer were eliminated ($q = 0 \text{ W m}^{-2} \text{ K}^{-1}$). Therefore, a radiative cooling coating with near-ideal selective emissive spectrum is proposed for all-day cooling.

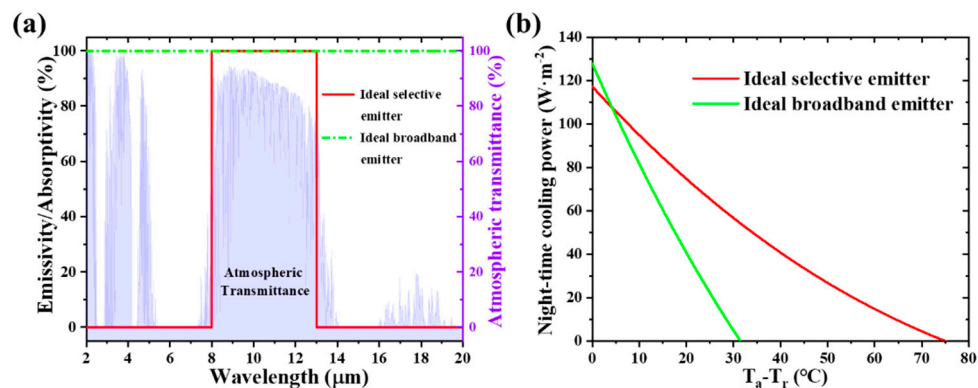


Figure 2. (a) IR emissivity/absorptivity of ideal broadband emitter and selective emitter; (b) Theoretical nighttime cooling performance of ideal broadband emitter and selective emitter with relative humidity 60%.

3.2. Optical Characteristics of the Radiative Cooling Coating

The infrared transmittivity spectra of the four functional nanoparticles used in this work are shown in Figure 3. The pressed-disk technique was used to measure the transmittance of functional nanoparticles. As a result, Figure 3 shows that SiO_x , mica, rare earth silicate, and molybdate functional nanoparticles have excellent infrared emissions of 8–10, 10, 10–12, and 12–13 μm , respectively.

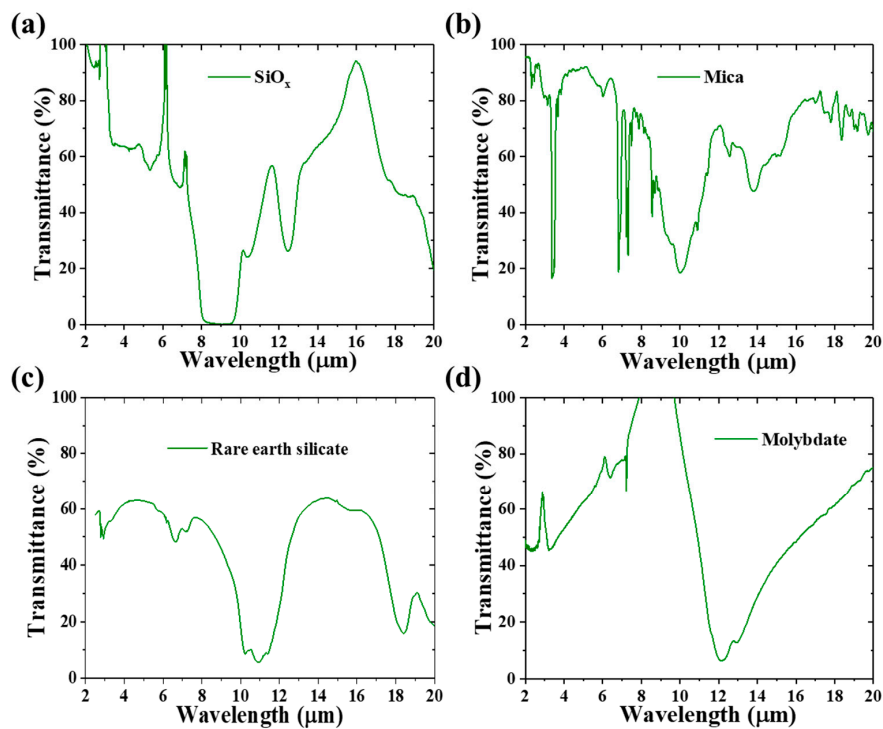


Figure 3. Transmittivity spectra of the functional nanoparticles: (a) SiO_x ; (b) mica; (c) rare earth silicate and (d) molybdate.

The absorptivity/emissivity spectra of the radiative cooling coating were experimentally characterized and are shown in Figure 4. As shown in Figure 4a, it is evident that P(VDF-HFP) coatings have strong and remarkably selective emissivity in the atmospheric window between 8–13 μm . Moreover, due to the addition of SiO_x , mica, rare earth silicate, and molybdate functional nanoparticles, the P(VDF-HFP) coatings can emit effectively within the entire atmospheric window. The overall thermal emissivity of the radiative cooling coating can reach up to 0.62. In addition, the radiative cooling coating can significantly cool 45 $^\circ\text{C}$ below the ambient temperature (27 $^\circ\text{C}$) with the absence of nonradiative heat exchange (Figure 4b).

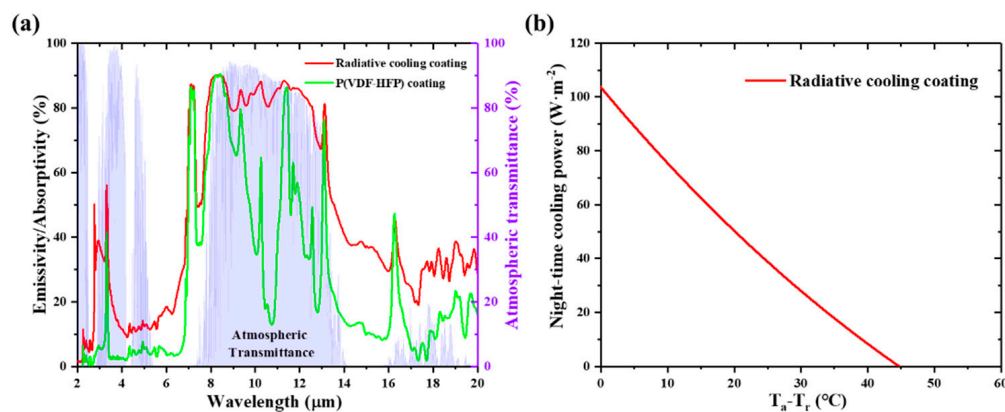


Figure 4. (a) IR emissivity/absorptivity of poly(vinylidene fluoride-co-hexafluoropropene) (P(VDF-HFP)) coating and radiative cooling coating; (b) Theoretical nighttime cooling performance of radiative cooling coating with relative humidity 60%.

3.3. Outdoor Experiments

Roof-top measurements were carried out on 23 and 29 July 2019 in Nanjing, China. The geographic location and weather conditions will affect the radiative cooling performance [19,20]. A clear day and low humidity are required for a high cooling power (P_{cooling}). To evaluate the cooling performance of the radiative cooling coating in a real environment, the rooftop measurements were carried out in clear summer weather, daytime and nighttime (relative humidity of 84% and 65%, respectively). The schematic and picture images of the test apparatus are shown in Figure 5a,b. It is worth noting that the temperature measurement point in the center of the box is different from the traditional one on the back of the radiator. In order to obtain a high P_{cooling} , the relative humidity (65%) of the clear summer night was chosen, and the result is presented in Figure 5c. The temperature of the radiative cooling coating dropped 4 ± 0.5 °C below the ambient air temperature, showing better cooling efficiency than Reference Sample 1 (commercial cooling coating) and Reference Sample 2. In agreement with the results discussed above, the cooling ability of the selective radiative cooling radiator is better than that of a broadband radiator (Reference Sample 1, see Figure S2).

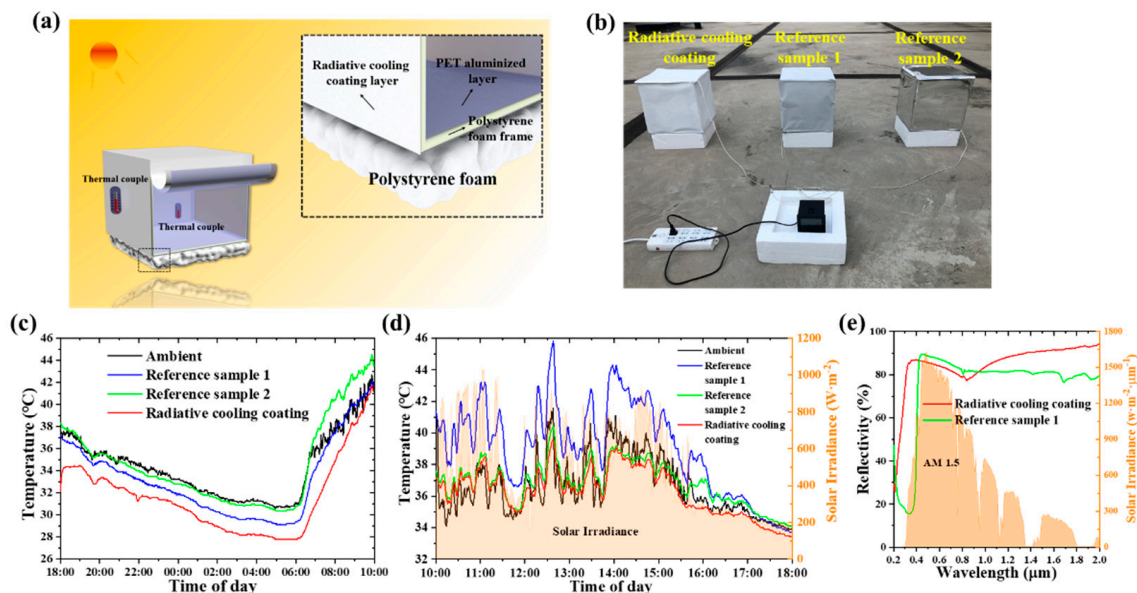


Figure 5. The rooftop measurement apparatus and the testing results: (a,b) The schematic and picture of the testing apparatus, respectively; (c,d) Nighttime (29 July 2019) and daytime (23 July 2019) test results of the rooftop measurements, respectively; (e) Solar reflectivity of the radiative cooling coating and commercial cooling coating.

In addition, Figure 5d shows that when over $800\text{--}1000\text{ W m}^{-2}$ of solar power was experienced by the samples, the commercial cooling coating (Reference Sample 1) reached a temperature higher than the ambient temperature for 4 ± 0.3 °C, whereas PET aluminized film (Reference Sample 2) and the radiative cooling coating can maintain 1 ± 0.2 °C below the ambient temperature (12:00–16:00). When the samples were not under direct sunlight, the temperatures of Reference Samples 1 and 2 remained a little higher than the ambient temperature, but the radiative cooling coating still remained a little lower than the ambient temperature (16:00–18:00). One reason for the low P_{cooling} was the high relative humidity (84%). The infrared transmittance of the atmosphere varies with the relative humidity of the environment. When the relative humidity is high, the micron-sized water drops in the atmosphere will scatter the infrared rays, obviously. The atmospheric scattering of infrared rays prevents the radiative cooling coating from radiating infrared directly to outer space for effective cooling. Hence, the relative humidity plays an important role in the cooling effect.

From the analysis above, it is clear that the radiative cooling coating on PET aluminized film has excellent actual cooling property in the nighttime, however, the daytime cooling effect is not obvious. The reason for this phenomenon is that the reflectance of PET aluminized film in the solar spectrum is not high enough to block the solar energy effectively (Figure S1c). As shown in Figure 5e, the reflectivity of the coatings on PET aluminized film is relatively low (75–90%). Furthermore, the absorption of solar radiation of the material can reach up to 0.16. If PET aluminized film is coated with an Ag layer to improve its reflection of sunlight, an effective daytime cooling effect would be achieved.

It should be noted that the test apparatus was fabricated with a volume of $40 \times 40 \times 40 \text{ cm}^3$ in this experiment, which was not sufficiently large for common utilization. The frame could be extended to form a larger model. This radiative cooling coating could maintain the cost below \$2 per m^2 , and have significant potential for market competition. The cost of the proposed selective radiator is expected to be highly competitive compared to traditional active cooling methods (for instance, air conditioning). Furthermore, the P(VDF-HFP) coatings are intrinsically resistant to weathering, fouling, and ultraviolet radiation, and capable of self-cleaning because of their hydrophobicity [11,21,22]. Hence, those properties enable the passive cooling material to maintain its optical performance and be used for a long time.

4. Conclusions

In summary, an affordable and efficient passive cooling coating was exploited in this study. The proposed selective radiative cooling coating can emit effectively within the entire atmospheric window, which can theoretically cool $45 \text{ }^\circ\text{C}$ below the ambient temperature, in the absence of nonradiative heat exchange. The developed selective radiative cooling coating allowed for a temperature reduction of $4 \pm 0.5 \text{ }^\circ\text{C}$ in the nighttime, which showed a better cooling effect than the commercial PET aluminized film and the commercial cooling coating. Importantly, due to its flexibility, low cost, and potential to be mass-manufactured, the coating can be applied to the market for large-scale application. The proposed cooling coating thus has enormous potential in changing cooling ways in industrial and residential applications.

Supplementary Materials: The following are available online at <http://www.mdpi.com/2079-6412/10/2/144/s1>, Figure S1: (a) EDS spectrum of PET aluminized film; (b) SEM image of PET aluminized film; (c) Solar reflectivity of PET aluminized film, Figure S2: (a) IR emissivity/absorptivity of the commercial cooling coating; (b) Theoretical nighttime cooling performance of commercial cooling coating with relative humidity 60%.

Author Contributions: Conceptualization, Z.F. and C.L.; methodology, M.C. and W.L.; investigation, M.C. and S.T.; writing—original draft preparation, M.C.; writing—review and editing, M.C., Z.F., C.L. and Z.X.; funding acquisition, C.L. and Z.X. All authors have read and agreed to the published version of the manuscript.

Funding: Financial support from the Natural Science Foundation of Jiangsu Province (BK20180714), special start-up funding from the Nanjing Tech University for the introduced talent, Priority Academic Program Development of the Jiangsu Higher Education Institutions (PAPD), the independent research topic of State Key Laboratory of Materials-Oriented Chemical Engineering (ZK201211), Qing Lan Project, Six Talent Peaks Project in Jiangsu Province (No. XCL-029), are gratefully acknowledged.

Conflicts of Interest: The authors declare no conflict of interest.

References

1. Kelso, J.K. *2011 Buildings Energy Data Book*; US Department of Energy: Washington, DC, USA, 2012.
2. Segar, C. Saudi energy mix: Renewables augment gas. *J. Int. Energy Agency* **2014**, *7*, 40–41.
3. Panchabikesan, K.; Vellaisamy, K.; Ramalingam, V. Passive cooling potential in buildings under various climatic conditions in India. *Renew. Sust. Energ. Rev.* **2017**, *78*, 1236–1252. [[CrossRef](#)]
4. An, C.; Su, J. Improved lumped models for transient combined convective and radiative cooling of multi-layer composite slabs. *Appl. Therm. Eng.* **2011**, *31*, 2508–2517. [[CrossRef](#)]
5. Safi, T.S.; Munday, J.N. Improving photovoltaic performance through radiative cooling in both terrestrial and extraterrestrial environments. *Opt. Express* **2015**, *23*, A1120–A1128. [[CrossRef](#)] [[PubMed](#)]

6. Zou, C.; Ren, G.; Hossain, M.M.; Nirantar, S.; Withayachumnankul, W.; Ahmed, T.; Bhaskaran, M.; Sriram, S.; Gu, M.; Fumeaux, C. Metal-loaded dielectric resonator metasurfaces for radiative cooling. *Adv. Opt. Mater.* **2017**, *5*, 1700460. [[CrossRef](#)]
7. Catalanotti, S.; Cuomo, V.; Piro, G.; Ruggi, D.; Silvestrini, V.; Troise, G. Radiative cooling of selective surfaces. *Sol. Energy* **1975**, *17*, 83–89. [[CrossRef](#)]
8. Orel, B.; Gunde, M.K.; Krainer, A. Radiative cooling efficiency of white pigmented paints. *Sol. Energy* **1993**, *50*, 477–482. [[CrossRef](#)]
9. Mahdavinejad, M.; Javanrudi, K. Assessment of ancient fridges: A sustainable method to storage ice in hot-arid climates. *Asian Cult. Hist.* **2012**, *4*, 133–139. [[CrossRef](#)]
10. Gao, M.; Han, X.; Chen, F.; Zhou, W.; Liu, P.; Shan, Y.; Chen, Y.; Li, J.; Zhang, R.; Wang, S.; et al. Approach to fabricating high-performance cooler with near-ideal emissive spectrum for above-ambient air temperature radiative cooling. *Sol. Energy Mater. Sol. Cells* **2019**, *200*, 110013. [[CrossRef](#)]
11. Mandal, J.; Fu, Y.K.; Overvig, A.C.; Jia, M.X.; Sun, K.R.; Shi, N.N.; Zhou, H.; Xiao, X.H.; Yu, N.F.; Yang, Y. Hierarchically porous polymer coatings for highly efficient passive daytime radiative cooling. *Science* **2018**, *362*, 315–318. [[CrossRef](#)] [[PubMed](#)]
12. Sakthisabarimoorathi, A.; Dhas, S.; Jose, M. Fabrication and nonlinear optical investigations of SiO₂@Ag core-shell nanoparticles. *Mater. Sci. Semicond. Process* **2017**, *71*, 69–75. [[CrossRef](#)]
13. Mrinmoy, G.; Mrinmoy, S. Effects of in-situ generated coinage nanometals on crystallization and microstructure of fluorophlogopite mica containing glass-ceramics. *J. Mater. Sci. Technol.* **2015**, *31*, 110–119.
14. Wenyan, Z.; Chunhua, L.; Yaru, N. Crystal structure and optical spectra of Er:NaLa_xYb_{9-x}(SiO₄)₆O₂ ($x = 0, 3, 5, 7, 9$) crystals prepared through a hydrothermal routine. *Adv. Mater. Res.* **2009**, *79*, 1711–1714.
15. Vidya, S.; Solomon, S.; Thomas, J.K. Synthesis, sintering and optical properties of CaMoO₄: A promising scheelite LTCC and photoluminescent material. *Phys. Status Solidi A Appl. Mat.* **2012**, *209*, 1067–1074. [[CrossRef](#)]
16. Hossain, M.M.; Gu, M. Radiative cooling: Principles, Progress, and Potentials. *Adv. Sci.* **2016**, *3*, 1500360. [[CrossRef](#)] [[PubMed](#)]
17. Raman, A.P.; Anoma, M.A.; Zhu, L.; Rephaeli, E.; Fan, S. Passive radiative cooling below ambient air temperature under direct sunlight. *Nature* **2014**, *515*, 540–544. [[CrossRef](#)] [[PubMed](#)]
18. Bao, H.; Yan, C.; Wang, B.X.; Fang, X.; Zhao, C.Y.; Ruan, X.L. Double-layer nanoparticle-based coatings for efficient terrestrial radiative cooling. *Sol. Energy Mater. Sol. Cells* **2017**, *168*, 78–84. [[CrossRef](#)]
19. Wang, W.M.; Fernandez, N.; Katipamula, S.; Alvine, K. Performance assessment of a photonic radiative cooling system for office buildings. *Renew. Energy* **2018**, *118*, 265–277. [[CrossRef](#)]
20. Guha, B.; Otey, C.; Poitras, C.B.; Fan, S.H.; Lipson, M. Near-field radiative cooling of nanostructures. *Nano Lett.* **2012**, *12*, 4546–4550. [[CrossRef](#)] [[PubMed](#)]
21. Bretzlaff, R.S.; Wool, R.P. Frequency shifting and asymmetry in infrared bands of stressed polymers. *Macromolecules* **1983**, *16*, 1907–1917. [[CrossRef](#)]
22. Arkema. New Fluoropolymer Latex Technology for Cool Materials Solutions Across an Expanded Color Space. Available online: <http://coolcolors.lbl.gov/assets/docs/PAC-2008-03-06/Arkema-slides.pdf> (accessed on 13 January 2020).

